COMPUTER NON-ITERATIVE DATA ACQUISITION OF PARTICLE TRAJECTORY IN A SPARK CHAMBER

by

Vladimir S. POLUŽANSKI [1,2*], ***Aleksandar D. ŽIGIĆ*** [2], ***Dragan S. KOVAČEVIĆ*** [2], ***and Boško D. NIKOLIĆ*** [1]

[1]School of Electrical Engineering, University of Belgrade, Belgrade, Serbia
[2]Electrical Engineering Institute 'Nikola Tesla', University of Belgrade, Belgrade, Serbia

Scientific paper
https://doi.org/10.2298/NTRP190125007P

This paper presents a novel non-iterative algorithm for charge particle localization in a spark chamber. Its performance is evaluated by computer simulations using the Monte Carlo simulation method and compared with the performance of an appropriate iterative algorithm. It is found that the proposed non-iterative algorithm performs significantly better, is easier to implement and requires less computational resources than the iterative algorithm.

Key words: spark chamber, spark localization, Monte Carlo method

INTRODUCTION

Detectors with an electrical output signal have the advantage of fast acquisition and display of data. They are especially convenient when geometric conditions are exactly known, for instance determining the number of scattered particles from a beam at a certain angle as a function of beam energy. However, such detection systems are not convenient for analysis of complex processes in which emissions of a large number of various particles are possible. In those cases visual type detectors are used, such as: fog chamber, bubble chamber, spark chamber and photographic emulsion [1-5].

A spark chamber represents a particle detector which was developed and often used between 1970. and 1980. Although, later it was partially superseded by other detectors, such as the drift chamber and silicon detectors, spark chambers still represent a valuable scientific instrument due to their characteristics such as high speed, selectivity in time and particle type, and for the possibility of computer acquisition of particle trajectory data. In the case of the simple spark chamber, the trajectory is obtained using a photographic recording. More complex spark chambers show the trajectory in real time, practically instantly. These chambers determine the particle location using piezoelectric acoustic detectors or using photomultipliers and a computer system with appropriate mathematical algorithms [6-8].

* Corresponding author; e-mail: vladimir.poluzanski@ieent.org

The aim of this work is to show a new advanced (non-iterative) algorithm for data acquisition of particle trajectory in a spark chamber and to compare its performance to the common iterative algorithm.

SPARK CHAMBER

A spark chamber consists of about twenty equal plate-like capacitors of rectangular shape. The plates are made of aluminum about 5 to 6 mm thick and their dimensions are several decimeters. The typical distance between plates is about 2 cm. Capacitors are placed vertically, one above the other. In this way, the overall detector height can be about 1 m. All capacitors are connected in parallel, so that there is equal voltage on each of them. The chamber with capacitors is filled with a mixture of neon and helium. The mixture is on at a higher than atmospheric pressure and slowly circulates among the plates [9-13].

Between the plates there is relatively high voltage, so that the electric field in dielectric is somewhat lower than the breakthrough value. Fast, subatomic particles when passing through the space between plates trigger the breakthrough by ionizing the gas mixture. As a result a spark occurs which can be seen by the naked eye and be photographed as well. The spark must be short-lived and it must not turn into an arc. That can be obtained by high output resistance of the generator [14-16].

The image of the subatomic particle trajectory is discrete and consists of about twenty sparks. Such a

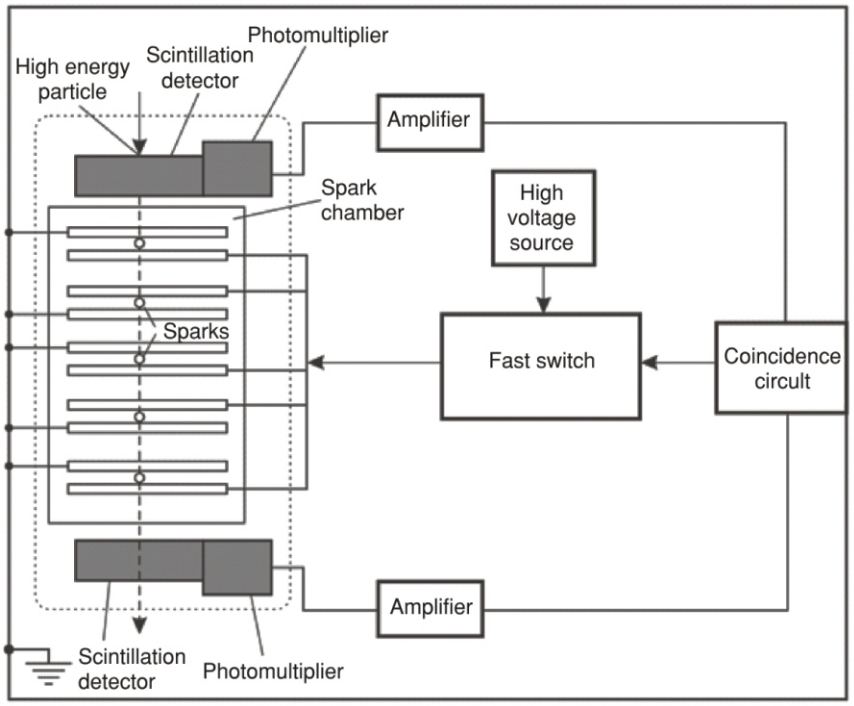

Figure 1. Spark chamber synchronized by using two scintillation detectors with photomultipliers

trajectory display is much rougher compared with recordings obtained by a bubble chamber. However, the advantage of a spark chamber is better synchronization, and a short active interval of recording. In this way, we can record some wanted rare events with high probability of a successful recording [17, 18].

Practical spark chambers have the structure shown in fig. 1. Apart from the vertically placed array of connected capacitors in parallel, above and below the chamber there is a scintillation detector with a photomultiplier. The passing of a subatomic particle through the chamber is detected by the appearance of two time-shifted electric pulses generated at the photomultiplier outputs. The time interval between these two pulses is equal to the time needed for the particle to pass through the chamber. The pulses from the photomultipliers are fed to timers and logical circuits. If the delay interval is equal to the expected, the activation of high voltage is done using logical circuitry. Such a synchronized spark chamber is secured from spontaneous triggering caused by cosmic radiation [19-21].

SPARK CHAMBER WITH AUTOMATIC TRACKING OF PARTICLE TRAJECTORY

As already explained, simple spark chambers use a photographic recording. More advanced ones use acoustic sensors and computers for recording. Localization of the point where the spark occurred is conducted by using the acoustic signal (short bang) caused by the spark (occurs by the explosion of the spark channel in which the pressure is around 2 MPa). For that purpose at each capacitor plane several piezoelectric microphones are placed. The number of microphones depends on whether the trajectory is determined in the plane or in space. The number is usually three, since in practice a simpler case of determination in the plane is used. When a spark occurs an acoustic signal is generated that excites all three microphones. A piezoelectric microphone generates a short electric pulse when the acoustic signal reaches it. The first electric signal is obtained by the microphone which is the closest to the place where the spark occurred, then signals from more distant microphones are obtained. Based on the knowledge of the chamber geometry, signal sequence and delay intervals among signals, it is possible to determine the spark location and henceforth the place where the particle has passed.

To give an explanation of the principle of how the automatic particle tracking is performed, fig. 2 shows the simplest cases of 1-D and 2-D point positioning in which the acoustic signal occurs.

Two acoustic detectors are located in points A and B which are placed at a known distance l. The acoustic signal occurs at point C which is on the straight line AB, at distance x from detector A, *i. e*. distance l-x from detector B. The velocity of the acoustic signal is c and is considered to be known. If the spark occurred at time $t = 0$, microphones at points A and B will record acoustic signals at time t_A and t_B which are

$$t_A \quad \frac{x}{c}, \; t_B \quad \frac{l \quad x}{c} \tag{1}$$

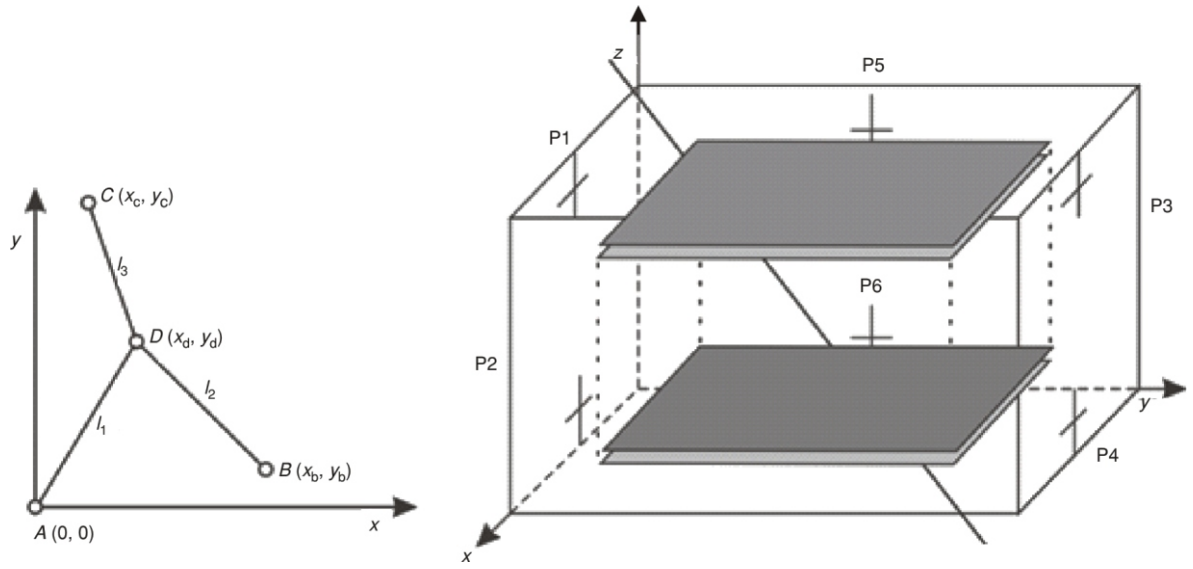

Figure 2. Illustration of 1-D and 2-D particle tracking

Using timers, the delay time interval is measured, $\Delta t_{BA} = t_B - t_A$, then using expression (1) we get the place x where the spark occurred

$$x \quad \frac{l}{2} \quad \frac{c}{2}\Delta t_{BA} \tag{2}$$

The most frequently used acquisition system for particle trajectory solves the problem in 2-D if one observes spark detectors that consists of plate capacitors with dielectric thickness much smaller than plate length. That justifies the representation of trajectory by its plane projection. For that purpose the triangulation procedure is used. To do that it is necessary to have three sensors at known co-ordinates $A(0, 0)$, $B(x_b, y_b)$, and $C(x_c, y_c)$. The source of the acoustic signal (spark) is located at point $D(x_d, y_d)$, whose co-ordinates x_d and y_d should be determined. The distance of point D corresponding to microphones is l1, l2, and l3, respectively. For these geometric relations we can use the following expressions

$$\begin{array}{cccc} l_1 & \sqrt{x_d^2 \quad y_d^2} & ct_1 \\ l_2 & \sqrt{(x_d \quad x_b)^2 \quad (y_d \quad y_b)^2} & ct_2 \\ l_3 & \sqrt{(x_d \quad x_c)^2 \quad (y_d \quad y_c)^2} & ct_3 \end{array} \tag{3}$$

The measurement system records time intervals among three signals, $\Delta t_{21} = t_2 - t_1$ and $\Delta t_{31} = t_3 - t_1$. Based on these expressions we get the system of two transcendent equations with two unknown values x_d and y_d

$$\begin{array}{cccc} l_2 \quad l_1 & \sqrt{(x_d \quad x_b)^2 \quad (y_d \quad y_b)^2} & \sqrt{x_d^2 \quad y_d^2} & c\Delta t_{21} \\ l_3 \quad l_1 & \sqrt{(x_d \quad x_c)^2 \quad (y_d \quad y_c)^2} & \sqrt{x_d^2 \quad y_d^2} & c\Delta t_{31} \end{array} \tag{4}$$

The solution of system (4) is carried out numerically by using an appropriate algorithm. In following chapter, a new advanced (non-iterative) algorithm for spark localization is proposed.

NON-ITERATIVE ALGORITHM FOR SPARK LOCALIZATION

Let us write expressions (3) and (4) as follows

$$\begin{array}{ccc} (x_d \quad x_a)^2 & (y_d \quad y_a)^2 & (ct_1)^2 \\ (x_d \quad x_b)^2 & (y_d \quad y_b)^2 & [c(t_1 \quad \Delta t_{21})]^2 \\ (x_d \quad x_c)^2 & (y_d \quad y_c)^2 & [c(t_1 \quad \Delta t_{31})]^2 \end{array} \tag{5}$$

Expression (5), represent 3 circles, with centers at respective sensor positions (points A, B, and C), passing through the spark source.

Any two of the circles in eq. (5) intersect, and the source is located at the intersecting line. Expression (6) for intersecting lines can be obtained by taking the difference of equations for circles with centers at points A and B and A and C. In the following expressions k_i are constants.

$$\begin{array}{cccc} 2x_d(x_b \quad x_a) & 2y_d(y_b \quad y_a) & 2c^2\Delta t_{21}t_1 & k_1 \\ k_1 & (x_b^2 \quad x_a^2) & (y_b^2 \quad y_a^2) & c^2\Delta t_{21}^2 \\ 2x_d(x_c \quad x_a) & 2y_d(y_c \quad y_a) & 2c^2\Delta t_{31}t_1 & k_2 \\ k_2 & (x_c^2 \quad x_a^2) & (y_c^2 \quad y_a^2) & c^2\Delta t_{31}^2 \end{array} \tag{6}$$

Expression (6) has the unknown variable t_1. By eliminating t_1 in expression (6), the line equation is obtained and given in eq. (7).

$$\begin{array}{cccc} k_4 x_d & k_5 y_d & k_6 & 0 \\ k_4 & \dfrac{x_b \quad x_a}{c^2\Delta t_{21}} & \dfrac{x_c \quad x_a}{c^2\Delta t_{31}} & \\ k_5 & \dfrac{y_b \quad y_a}{c^2\Delta t_{21}} & \dfrac{y_c \quad y_a}{c^2\Delta t_{31}} & \\ k_6 & \dfrac{k_1}{c^2\Delta t_{21}} & \dfrac{k_2}{c^2\Delta t_{31}} & \end{array} \tag{7}$$

Let us assume

$$y_d \quad A, A \quad R \tag{8}$$

Now, we have from eqs. (7) and (8)

$$\begin{array}{ccc} x_d & k_7 & k_8 A \\ & k_7 & \dfrac{k_6}{k_4} \\ & k_8 & \dfrac{k_5}{k_4} \end{array} \tag{9}$$

By putting eqs. (8) and (9) in eq. (6), the value of t_1 is obtained in terms of A and constants (eq. 10)

$$\begin{array}{ccc} t_1 & k_9 & k_{10} A \\ k_9 & \dfrac{k_1}{2c^2 \Delta t_{21}} & \dfrac{x_b \quad x_a}{c^2 \Delta t_{21}} \; k_7 \\ k_{10} & \dfrac{x_b \quad x_a}{c^2 \Delta t_{21}} & \dfrac{y_b \quad y_a}{c^2 \Delta t_{21}} \end{array} \tag{10}$$

Now we have x_d, y_d, and t_1 obtained in terms of A and constants. By substituting these values in eq. (5) a quadratic equation in A as in eq. (11) is obtained.

$$\begin{array}{cccc} k_{11} A^2 & k_{12} A & k_{13} & 0 \\ k_{11} & k_8^2 & c^2 k_{10}^2 & 1 \\ k_{12} & 2k_7 k_8 & 2k_8 x_a & 2y_a \quad 2k_9 k_{10} c^2 \\ k_{13} & k_7^2 & 2k_7 x_a & c^2 k_9^2 \quad x_a^2 \quad y_a^2 \end{array} \tag{11}$$

The solution of eq. (11) gives two values of A. By substituting A in eqs. (8)-(10), two sets of values for x_d, y_d, and t_1 are obtained. Out of these two sets, one is an accepted solution and the other is rejected from a practical standpoint. It may be due to either t_1 being negative or x_d and y_d being negative or outside of the dimensions of the capacitor [22].

SIMULATION RESULTS OF COMPARISON BETWEEN THE ITERATIVE AND NON-ITERATIVE ALGORITHM

For the iterative method the trust-region dogleg algorithm is used. This algorithm is a variation of the Powell dogleg method described in [23] which is similar to the method described in [24]. Simulations are carried out in MatLab using the non-linear system equations solver- *fsolve* function.

Non-iterative method simulations are carried out by a software tool, written in the C# programming language, which implements the algorithm described in the previous section.

The Monte Carlo method is used for random generation of spark locations, while sensor positions remain the same. The number of simulations is 1000.

For the simulation, a plate-like capacitor of rectangular shape with dimensions of 0.3 m 0.2 m 0.02 m is considered. Each of the 3 sensors is placed on a different side of the capacitor. The sensors' co-ordinates are: $x_a = 0$ m, $y_a = 0.15$ m, $x_b = 0.12$ m, $y_b = 0$ m, $x_c = 0.3$ m, $y_c = 0.1$ m, $z_a = z_b = z_c = 0.01$ m. The considered sound velocity through the dielectric is 345 ms^{-1}.

For both considered methods, which calculate the spark location in 2-D space, input values for arrival time differences t_{BA} and t_{CA} are derived from 3-D space that corresponds to real conditions.

Let us assume that the spark location, for every iteration of the Monte Carlo method, has a nominal value of x_d and y_d. Simulation results for spark localization by the iterative method are denoted as x_{ir}, y_{ir} and by non-iterative as x_{nr}, y_{nr}. Changes of the result with respect to the nominal value are: $x_{ir} = |x_{ir}\text{-}x_d|$, $y_{ir} = |y_{ir}\text{-}y_d|$, $x_{nr} = |x_{nr}\text{-}x_d|$ and $y_{nr} = |y_{nr}\text{-}y_d|$.

The simulation flow chart is presented in fig. 3, while simulation results for iterative and non-iterative methods are given in tab. 1.

DISCUSSION

Based on analysis of obtained simulation results, it has been observed that non-iterative method performed significantly better than iterative method. To be specific, the non-iterative method gave values by two orders of magnitude lower than the iterative method for parameters from table rows 5 to 10 (see tab. 1). Inherently, the non-iterative method gave results in one iteration, while the iterative method needed six iterations on average to produce a solution. The non-iterative method did not have any rejected solutions, contrary to the iterative method which had approximately five percent of rejected solutions.

It was also observed that maximum values of x_{ir}, y_{ir}, x_{nr}, and y_{nr} occur when the nominal spark location values are close to capacitors edges. Most of the rejected values for the iterative method happened in the same case.

Using the non-iterative method the combined measurement uncertainty of spark localization is reduced by 2 % [25-28].

CONCLUSIONS

The goal of the presented research was to describe a novel algorithm for spark localization and to compare it to the commonly used algorithm.

It is shown that the proposed non-iterative algorithm for spark localization performed significantly better than the common iterative algorithm. Performance analysis was carried out using the Monte Carlo computer simulation. Based on the presented results and taking into consideration that the proposed non-iterative algorithm is easier to implement in any programming language and requires less computational resources than the iterative algorithm, the use of the non-iterative algorithm for spark localization is recommended.

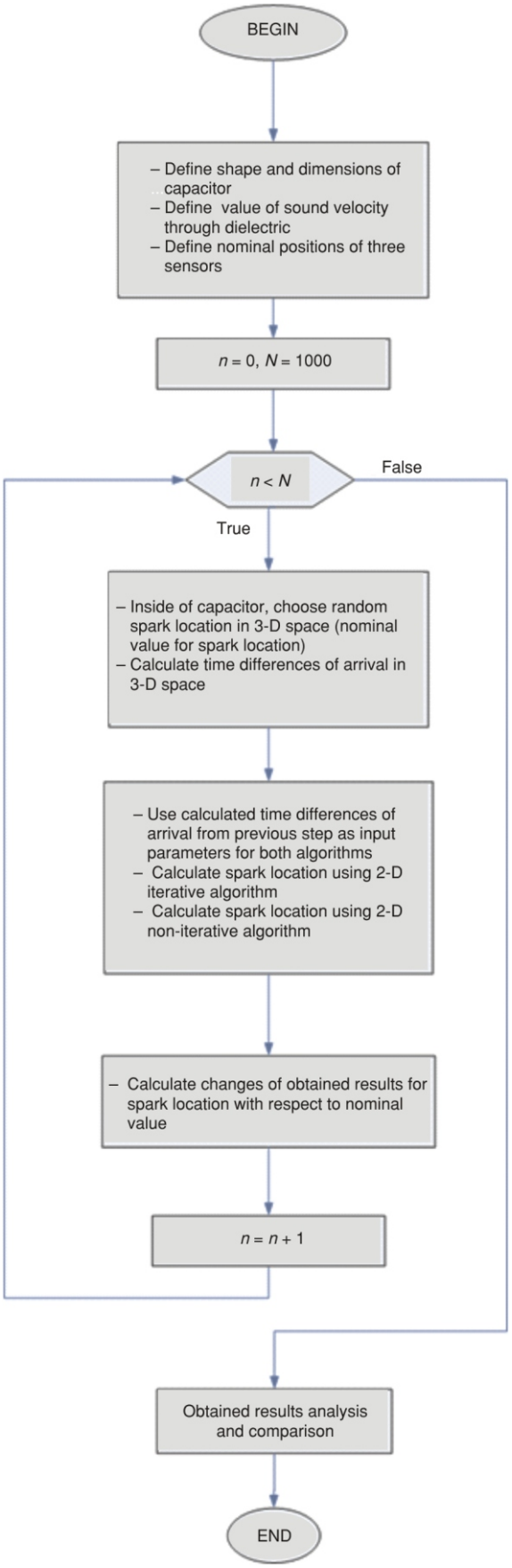

Figure 3. Simulation flow chart

Table 1 Simulation results for iterative and non-iterative methods

Row number	Parameter	Simulation results	
		Iterative method	Non-iterative method
1	Maximum number of iterations	21	1
2	Minimum number of iterations	4	
3	Average number of iterations	6	
4	Number of rejected solutions	54	0
5	Maximum value of x_{ir} [m]	0.2996	0.0039
6	Minimum value of x_{ir} [m]	0	0
7	Average value of x_{ir} [m]	0.0781	0.0001
8	Maximum value of y_{ir} [m]	0.1974	0.0028
9	Minimum value of y_{ir} [m]	0	0
10	Average value of y_{ir} [m]	0.0433	0.0001

The presented non-iterative algorithm does not solve the problem of spark localization in 3-D space, which can be of significance if nuclear particles are obtained by reactions occurring on the trajectory of the original particle. This problem requires further research.

ACKNOWLEDGMENT

This work was supported by the Ministry of Education, Science and Technological Development of the Republic of Serbia under contract no. TR 33017.

AUTHORS' CONTRIBUTIONS

Simulations were made by V. S. Polužanski. Simulations were carried out by V. S. Polužanski and A. D. Žigić under supervision and guidelines of D. S. Kovačević and B. D. Nikolić. All authors discussed the results. The manuscript was written by V. S. Polužanski and A. D. Žigić. D. S. Kovačević, and B. D. Nikolić reviewed the manuscript. Figures were prepared by V. S. Polužanski. V. S. Polužanski and A. D. Žigić checked the manuscript and added corrections.

REFERENCES

[1] Wilkinson, D. H., Ionization Chambers and Counters, Cambridge University Press, Cambridge, UK, 1950
[2] Wilkinson, D. H., The Geiger Discharge Revisited Part I: The Charge Generated, *Nuclear Inst. and*

Methods in Physics Research, A, 321 (1992), 1-2, pp. 195-210
[3] Munir, M., *et al*., Design and Development of a Portable Gamma Radiation Monitor, *Review of Scientific Instruments, 80* (2009), 7, 073101
[4] Wilkinson, D. H., The Geiger Discharge Revisited Part II. Propagation, Nuclear Instruments and Methods in Physics Research, Section A: Accelerators, Spectrometers, *Detectors and Associated Equipment, 383* (1996), 2-3 pp. 516-522
[5] Wilkinson, D. H., The Geiger Discharge Revisited Part III. Convergence, Nuclear Instruments and Methods in Physics Research, Section A: Accelerators, Spectrometers, *Detectors and Associated Equipment, 383* (1996), 2-3, pp. 523-527
[6] Osmokrović, P., Fundamentals of Nuclear Physics, Academic Mind, 2008, pp. 310-412 (in Serbian), Belgrade, Serbia
[7] Osmokrović, P., *et al*., Mechanism of Electrical Breakdown of Gases for Pressures from 10-9 to 1 bar and Inter-Electrode Gaps from 0.1 to 0.5 mm, *Plasma Sources Science and Technology, 16* (2007), 3, pp. 643-655
[8] Pejović, M. M., *et al*., Experimental Investigation of Breakdown Voltage and Electrical Breakdown Time Delay of Commercial Gas Discharge Tubes, *Japanese Journal of Applied Physics, 50* (2011), 8, pp. 086001-5
[9] Barclay, D., Improved Response of Geiger Muller Detectors, *IEEE Transactions on Nuclear Science, 33* (1986), 1, pp. 613-616
[10] Wilkinson, D. H., Geiger Discharge Revisited: Part IV. The Fast Component, Nuclear Instruments and Methods in Physics Research, Section A: Accelerators, Spectrometers, *Detectors and Associated Equipment, 435* (1999), 3, pp. 446-455
[11] Arbutina, D., *et al*., Aging of the Geiger-Muller Counter Due to Particle Conductance in an Insulating Gas, *Nucl Technol Radiat, 32* (2017), 3, pp. 250-255
[12] Osmokrović, P., *et al*., Reliability of Three-Electrode Spark Gaps, *Plasma Devices and Operations, 16* (2008), 4, pp. 235-245
[13] Perazić, L. S., *et al*., Application of an Electronegative Gas as a Third Component of the Working Gas in the Geiger-Muller Counter, *Nucl Technol Radiat, 33* (2018), 3, pp. 268-274
[14] Vagle, O., *et al*., A Simple and Efficient Active Quenching Circuit for Geiger-Mueller Counters, Nuclear Instruments and Methods in Physics Research, Section A: Accelerators, Spectrometers, *Detectors and Associated Equipment, 580* (2007), 1 Special Issue, pp. 358-361
[15] Vujisić, M., *et al*., A Statistical Analysis of Measurement Results Obtained from Nonlinear Physical Laws, *Applied Mathematical Modeling, 35* (2011), 7, pp. 3128-3135
[16] Meric, I., *et al*., Enhancement of the Intrinsic Gamma-Ray Stopping Efficiency of Geiger-Mueller Counters, Nuclear Instruments and Methods in Physics Research, Section A: Accelerators, Spectrometers, *Detectors and Associated Equipment, 696* (2012), Dec., pp. 46-54
[17] Milanović, Z., *et al*., Calculation of Impulse Characteristics for Gas-Insulated Systems with Homogenous Electric Field, *IEEE Transactions on Dielectrics and Electrical Insulation, 19* (2012), 2, pp. 648-659
[18] Weigel, F., Keuth, H., Patentschrift 1 2 99 357 Magnetischer Nutverschluss fur Elektrische Maschinen, PATENTAMT Bundesrepublik Deutschland, 1970
[19] Kartalović, N., M., *et al*., The Determination of the Mean Value of the Non-Homogenous Background Radiation and the Measurement Uncertainty Using Welch-Satterthwaite Equation, *Nucl Technol Radiat, 32* (2017), 4, pp. 371-374
[20] Čaršimamović, A., S., *et al*., Low Frequency Electric Field Radiation Level Around High-Voltage Transmission Lines and Impact of increased Voltage Values on the Corona Onset Voltage Gradient, *Nucl Technol Radiat, 33* (2018), 2, pp. 201-207
[21] Stanković, K., *et al*., Surface-Time Enlargement Law for Gas Breakdown, *IEEE Transactions on Dielectrics and Electrical Insulation, 15* (2008), 4, 4591220, pp. 994-1005
[22] Polužanski, V., *et al*., Algorithm for Calculating Influence of Power Transformer Oil Temperature Change on the Accuracy of All-Acoustic Non-Iterative Partial Discharge Localization, *FME Transactions, 46* (2018), 2, pp. 183-193
[23] Powell, M. J. D., A Fortran Subroutine for Solving Systems of Nonlinear Algebraic Equations, Numerical Methods for Nonlinear Algebraic Equations, H. M. Stationery Office, P. Rabinowitz, ed., 1970, Ch.7
[24] More, J. J., *et al*., User Guide for MINPACK 1, Argonne National Laboratory, Argonne, Ill., USA, Rept. ANL-80-74, 1980
[25] Vujisić, M., *et al.*, A Statistical Analysis of Measurement Results Obtained from Nonlinear Physical Laws, *Applied Mathematical Modeling, 35* (2011), 7, pp. 3128-3135
[26] Stanković, K. D., *et al*., Influence of Tube Volume on Measurement Uncertainty of GM Counters, *Nucl Technol Radiat, 25* (2010), 1, pp. 46-50
[27] Stanković, K., *et al*., Statistical Analysis of the Characteristics of Some Basic Mass-Produced Passive Electrical Circuits Used in Measurements, *Measurement: Journal of the International Measurement Confederation, 44* (2011), 9, pp. 1713-1722
[28] Kovačević, A. M., *et al*., Uncertainty Evaluation of the Conducted Emission Measurements, *Nucl Technol Radiat, 28* (2013), 2, pp. 182-190

Received on January 25, 2019
Accepted on February 8, 2019

**Владимир С. ПОЛУЖАНСКИ, Александар Д. ЖИГИЋ,
Драган С. КОВАЧЕВИЋ, Бошко Д. НИКОЛИЋ**

КОМПЈУТЕРСКА НЕИТЕРАТИВНА АКВИЗИЦИЈА ПОДАТАКА О ТРАЈЕКТОРИЈИ ЧЕСТИЦЕ У ВАРНИЧНОЈ КОМОРИ

У раду је представљен нови неитеративни алгоритам за одређивање положаја наелектрисане честице у варничној комори. Перформансе овог алгоритма су процењене компјутерским симулацијама користећи Монте Карло методу и упоређене са перформансама одговарајућег итеративног алгоритма. Утврђено је да предложени неитеративни алгоритам ради значајно боље, лакши је за имплементацију и захтеву мање компјутерских ресурса од итеративног алгоритма.

Кључне речи: варнична комора, одређивање положаја наелектрисане честице, Монте Карло метода